Anthropomorphic Walking Robot: Design and Simulation

M. Polishchuk
Associate Professor
National Technical University of Ukraine
Department of Information Systems and Technologies
Ukraine

M. Tkach
Associate Professor
National Technical University of Ukraine
Department of Information Systems and Technologies
Ukraine

A. Stenin
Professor
National Technical University of Ukraine
Department of Information Systems and Technologies
Ukraine

The current stage of development of robotic systems is characterized by the use of anthropomorphic robot designs, the functions of which are as close as possible to human capabilities. This trend is explained by the need to give robots universal capabilities when performing various technological operations. The article proposes a fundamentally new design of a walking robot and describes a model of its functioning. This design allows the robot to move in an angular coordinate system, which is typical for humans. The main motivation for creating such a robot is to reduce the number of drives for the kinematic chain of the walking mechanism.
The article presents the results of mathematical modeling and recommendations for the design of anthropomorphic walking mechanisms. The engineering formulas and diagrams presented in the article for calculating force loads make it possible to create various modifications of walking robots that have the property of adapting to an arbitrary surface topology for moving a mobile robot. The economic effect is achieved by reducing the number of electric motors for the robot's leg joints and, consequently, by reducing the total cost of the walking robot.

***Keywords**: walking mechanisms, industrial robots, anthrop–omorphic devices, robots' design*

1. INTRODUCTION

Anthropomorphic designs of mobile robots make it possible to achieve the functions' versatility. However, it should be noted that anthropomorphic walking mec–hanisms have a lower carrying capacity than other transmissions, such as wheeled or tracked ones. This disadvantage is explained by the need for separate motors for each joint of the leg of a walking robot. In addition, the presence of many electric motors limits the energy resource of autonomous power sources. There–fore, creating a walking mechanism with a minimum number of electric motors is necessary.

This article proposes an anthropomorphic leg mec–hanism for a mobile robot with one eclectric motor and two hermetic gas chambers (Patent UA 125121). These gas chambers perform the function of energy recovery when the robot walks. Such a minimum number of drives, together with the original kinematics of the robot's leg, is sufficient for walking when performing transport operations. The article also provides analytical formulas and diagrams for calculating the parameters of a new walking mechanism. The functioning of the proposed walking robot, which contains four anthropo–morphic legs, is simulated. The main motivation for creating such a robot is to minimize the walking mec–hanism drives to perform transport operations. This leads to a significant reduction in the cost of a mobile walking robot and a simultaneous increase in its car–rying capacity as a vehicle.

2. PREREQUISITES AND MEANS FOR SOLVING THE PROBLEM

The problem with creating walking robots is the need to ensure their stable position when moving on surfaces with different topologies. The presence of separate drives for each articulation is quite acceptable when power is supplied through cables, but there are more effective solutions for mobile robots using autonomous power sources that have limited energy resources. Cur–rently, experimental models of walking mechanisms have been developed, each of which has certain ad–vantages and disadvantages. Known walking robot [1], made in the form of a kinematic chain of hinged levers and drives in each of these hinges. A bipedal walking robot is also known [2], in which electric motors for driving joints are located on each leg of the robot. The walking mechanisms of this robot are as close as possible to an anthropomorphic device (from the Eng–lish anthropomorphous - in shape, the device is similar to a person, his body). Thanks to the many joints (hin–ges) of the walking mechanism, the robot has an arbitrary orientation in space. However, as in the previous case, the robot does not provide energy savings for an autonomous power source due to the need for the same set of drives.

In the walking device [3], each of the articulated joints has a drive that performs the rotational move–ment. Despite the increased reliability of the foot sup–port of

Received: October 2022, Accepted: November 2022
Correspondence to: Dr Mikhail Polishchuk, Associate Professor, National Technical University of Ukraine "Igor Sikorsky Kyiv Polytechnic Institute", Kyiv, Ukraine, E-mail: borchiv@ukr.net
doi: 10.5937/fme2204724P

this device, there needs to be a separate drive for each swivel to contribute to saving the energy resource of an autonomous power source. In [4, 5], a dynamic model of a walking mechanism was proposed. This robot has only two degrees of freedom, but it can step forward and backward, rotate at an arbitrary angle, go around obstacles and even climb stairs. This design is interesting from the point of view of minimizing the number of drives. An estimate of the mechanical model of a bipedal walking robot is also presented in [6]. Studies [7, 8] are of interest from the point of view of optimal control of anthropomorphic structures. The original designs of walking feet are presented in [9, 10, 11], but without considering the designs of the actual legs of the robot.

The analysis of models of anthropomorphic robots presented in [12] illustrates the possibilities of machine learning for walking robots based on the algorithms of bionic structures. In [13], the designs of walking robots with four and six legs are proposed. However, in these works, there are no recommendations for improving the energy efficiency of walking robots by reducing the drives. The original bionic model of a miniature walking robot was proposed in [14], where the drives for the six legs of the robot were minimized. Studies [15-17] consider the construction of bipedal walking robots both in the form of anthropomorphic structures, as well as in the form of six-legged Hexapods [18, 19]. How–ever, in both cases, each leg joint of the robots is equipped with a separate drive (engine), which increases the energy costs from the autonomous power sources of the robots. The undisputed leader in the creation of walking robots is the Boston Dynamics laboratory [20], but the cost of these robots is still too high. The possibility of integrating the drives of a walking robot is presented in [21]. Still, since the legs of the robot are made of elastic material in the form of corrugated chambers under pressure, such a robot has a low load capacity.

Thus, the above analysis of technical solutions and research shows that the task of synthesizing a mobile walking robot of an anthropomorphic design with a minimum number of drives remains relevant.

3. FORMULATION OF THE PROBLEM

To reduce energy costs and save resources of autono–mous power sources, it is necessary to create an anthro–pomorphic walking robot with a minimum but a sufficient number of drives for each leg of the robot. In addition, it is necessary to develop analytical depen–dencies for calculating the parameters of a walking robot, which will allow engineers in the field to design similar walking mechanisms for mobile robots.

As shown below, the solution to this problem is possible even with one electric motor for each leg of the robot in combination with the original kinematic scheme.

3.1 SOLUTION OF THE PROBLEM UNDER CONSI–DERATION

The main motivation of this research is to create an anthropomorphic walking mechanism with a high load capacity with a minimum number of motors for the legs of the robot. The consequence of this property is a significant reduction in the cost of a walking robot while saving the energy resources of autonomous power sources of the robot. The technical novelty of the pro–posed engineering solutions lies in a fundamentally new design of a mobile walking robot [22], and graphical and analytical dependencies display the scientific no–velty for calculating the parameters and modeling the specified robot.

3.2 Walking robot design

Figure 1 shows a 3D model of a walking robot in a quarter section. The robot's body contains a parallel upper platform and a lower platform, which are con–nected by a rolling bearing in the form of a bearing. An electric motor is fixed on the upper platform, which imparts rotation to the lower platform through an internal gear train. When the electric motor is turned on or reversed, one platform rotates relative to the other platform; that is, the robot rotates when the direction of movement changes.

The robot has four legs, two of which, namely, the left front leg and the right rear leg, are mounted on the upper platform, and the right front leg and the left rear leg are mounted on the lower platform. The legs of the robot work in pairs and diagonally to the body. When the robot leans on the left front leg and the right back leg, the right front leg and the left back leg bend at the knee joints and move as shown below. Also, a teles–copic arm and its rotation module are installed on the upper platform. These devices form a manipulator with two degrees of movement: ±R, and $\pm\varphi$ perform various technological tasks. The power supply and the robot control unit are also installed on the upper platform.

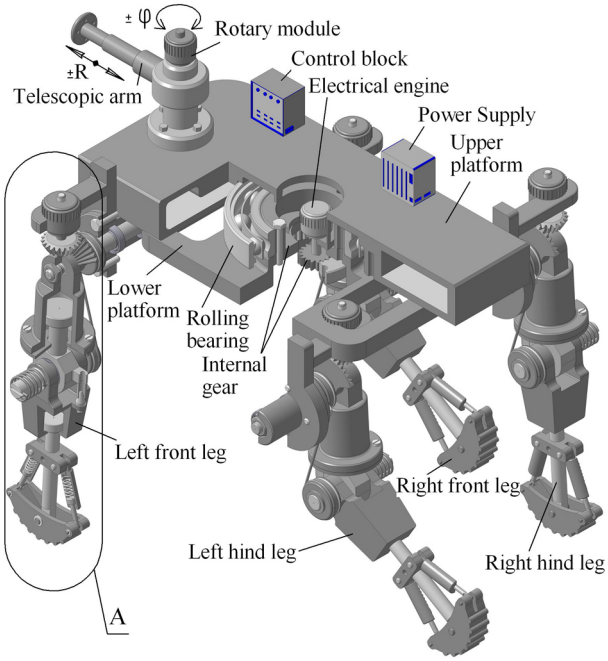

Figure 1. Anthropomorphic walking robot (3D model in quarter section)

The robot's leg structures are the same (see Figure 2), and each of them contains a thigh, a lower leg, and a foot, which are kinematically connected to each other. The leg thigh is made in the form of a piston cylinder,

which forms a gas-sealed chamber in the form of cavity "B", which is pre-filled with compressed gas. The upper part of this piston cylinder is mounted on a shaft with bearings and receives rotation drive from an electric motor through a gear wheel and a bevel gear. The rod of the piston cylinder is fixed on the leg knee shaft, on which the lower leg is also fixed. The lower leg, like the thigh, is made in the form of a piston cylinder, which forms a gas-sealed chamber in the form of cavity "C", also pre-filled with compressed gas.

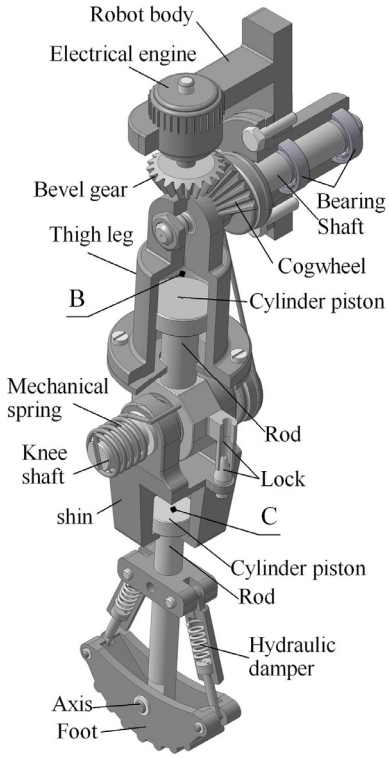

Figure 2. Walking robot leg design (see item "A" in Figure 1)

On the rod of the piston cylinder of the lower leg, hydraulic dampers and the foot of the robot are ins–talled. These dampers are necessary to dampen shock loads when the robot walks. In addition, the knee shaft is connected to a mechanical spring for leg extension while walking and has a lock for fixing the lower leg relative to the leg thigh.

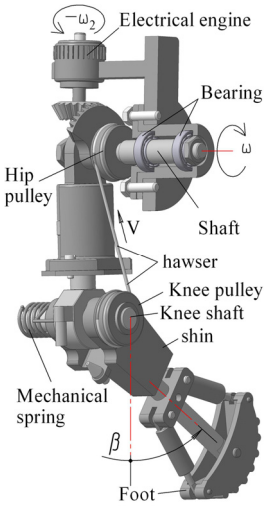

Figure 3. The leg of the robot in a bent position (when the lower leg is rotated to an angle *β*)

Figure 3 shows the leg in a bent position. The bending of the leg, or rather the rotation of the lower leg at an angle β, is carried out with the help of a cable transmission in the form of a thigh pulley fixed on the upper shaft, and a cable connected to the pulley, which is fixed on the leg knee shaft.

When the electric motor is reversed with an angular velocity - ω through a bevel gear, the femoral shaft rotates with an angular velocity ω. As a result, the thigh rotates, and the lower leg bends through the angle β. This movement is transmitted from the electric motor through the femoral pulley and the knee shaft pulley, which are connected by a cable moving at a speed V.

3.3 Robot leg movement

The movement of the walking robot is carried out as follows. The legs of the robot rotate in pairs and dia–gonally to the robot's body. Since the construction of all legs is the same, as an example, consider the movement of the left front leg, as shown in Figure 4.

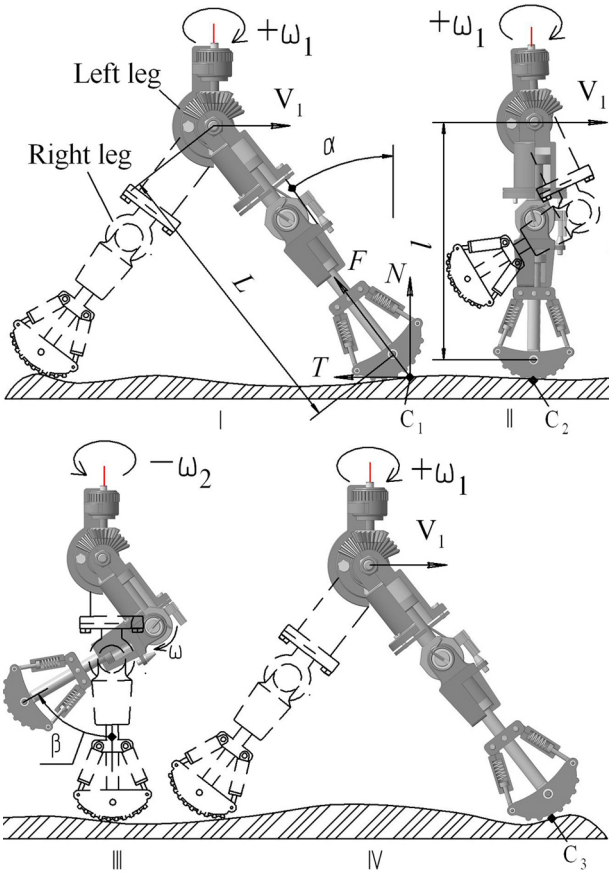

Figure 4. Stages of movement of the legs of a walking robot

At the first stage **I**, when the electric motor is turned on (see also Figure 2 and Figure 3), it rotates the leg of length L through an angle α around the point C_1 with an angular velocity through a bevel gear. At the same time, under the action of the weight of the robot, the gas in the sealed chambers of the thigh and lower leg (namely, in chambers "B" and "C" of the piston cylinders) is compressed to a certain pressure. The length of the robot's leg decreases from L to l, and the robot moves with linear speed V_1. The leg assumes the position of stage **II** at point C_2. With further movement of the robot

at stage **III** and with the reverse of the electric motor with an angular velocity - ω, the leg's shin through a cable transmission (as shown in Figure 3) with an angular velocity is bent through an angle β. This twists the mechanical spring on the knee shaft. With further movement of the robot at stage **IV**, the reverse of the electric motor is switched on again with an angular velocity $+\omega_1$. The mechanical spring on the shaft of the knee of the leg rotates the lower leg to its original position, and the expansion of the compressed gas in the piston cylinders of the thigh and lower leg straightens the leg to the initial position of length L at point C_3. This is how the robot moves one step. Further, the cycle of movement is repeated when the legs of the robot move in pairs and along the diagonal of its body.

Thus, due to gas compression in chambers "B" and "C" of the piston cylinders, the leg length under the influence of the robot's weight force decreases by the value $L - l = \delta$ to ensure the rectilinear movement of the robot, and the cable transmission, when the electric motor is reversed, bends under the action of a mecha–nical spring on the knee shaft unbends the leg of the robot. At the same time, chambers "B" and "C" of the piston cylinders of the thigh and lower leg, when the compressed gas expands, perform the function of recu–perating the energy of the compressed gas and straig–htening the robot's leg to its original position. As a result, it seems possible to carry out the movement of the robot's leg only due to one electric motor, two sealed gas chambers, and cable transmission. Unlike the tec–hnical solutions discussed above (See Section 2), when a separate motor is used for each leg joint, the proposed leg design can significantly reduce the cost of the robot and achieve savings in autonomous power sources.

4. SIMULATION OF THE FUNCTIONING OF THE LEG OF A WALKING ROBOT

For the possibility of designing such walking mecha–nisms, below are the first analytical formulas created for calculating the design parameters of the robot's gas chambers of the thigh and lower leg. Next, the simu–lation of the dynamics of the movement of the robot is performed, graphs of the change in kinematic charac–teristics are proposed, and formulas for the stability of the walking robot are given.

5.1 Determining the parameters of the gas chambers

During the movement of the robot, at the points of contact of the supporting leg with the surface, a normal reaction N occurs (see Figure 4, stage 1) and a hori–zontal friction force T, which are determined by the formulas: $N = G/2$; $T = fN = fG/2$, where G – is the total mass of the robot; f – is the coefficient of friction between the foot and the moving surface.

At an arbitrary moment in time, a force will act along the leg

$$F = N\cos\alpha + T\sin\alpha = G(\cos\alpha + f\sin\alpha)/2 \qquad (1)$$

where: α - is the angle between the axis of the leg and the vertical; ($-45° \le \alpha \le 45°$). In the initial position at the value $\alpha = \alpha_0 = -45°$ force F along the leg is equal to $F = F_0 = G(\cos 45° - f \sin 45°)/2 = G(1-f)\sqrt{2}/4$. This force corresponds to the initial values of gas pressure in the sealed chambers of the femur p_{01} and lower leg p_{02}, respectively:

$$p_{o1} = \frac{F_o}{\pi D^2/4} = \frac{G(1-f)\sqrt{2}}{\pi D^2},$$
$$p_{o2} = \frac{F_o}{\pi d^2/4} = \frac{G(1-f)\sqrt{2}}{\pi d^2}. \qquad (2)$$

At the time when the angle $\alpha = 0$, equalities take place:

$$F = F_1 = G\cdot 2;\ p_{11} = \frac{F_1}{\pi D^2/4} = \frac{2G}{\pi D^2};$$
$$p_{12} = \frac{F_1}{\pi d^2/4} = \frac{2G}{\pi d^2}, \qquad (3)$$

where: gas pressures in sealed chambers “B” and “C”, respectively: femur p_{11} and tibia p_{12} at an arbitrary point in time; D, d are the diameters of the femur and tibia piston cylinders, respectively (see Figure 5).

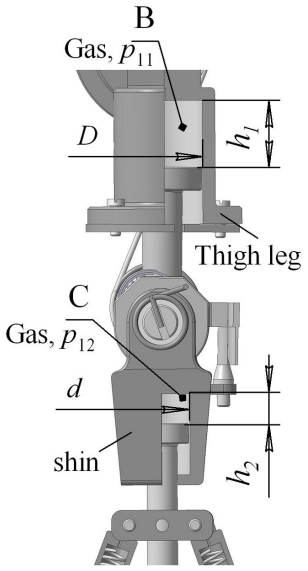

Figure 5. Parameters of the gas chambers of the thigh and lower leg of the robot's legs

According to the Boyle-Mariotte law, in an isother–mal process, the equalities will be fulfilled:

$$p_{o1}\frac{\pi D^2}{4}h_1 = p_{11}\frac{\pi D^2}{4}(h_1 - \delta/2);$$
$$p_{o2}\frac{\pi d^2}{4}h_2 = p_{12}\frac{\pi d^2}{4}(h_2 - \delta/2), \qquad (4)$$

where: h_1, h_2 are the lengths of the thigh and shins chambers; $\delta = L - L\cos 45°$ – change in the length of the supporting leg during the robot's movement. From equ–ation (4) we determine the lengths of the gas chambers of the thigh and lower leg, respectively:

$$h_1 = \frac{p_{11}\delta}{2(p_{11} - p_{01})} = \frac{2\delta}{2(2-(1-f)\sqrt{2})};$$
$$h_2 = \frac{p_{12}\delta}{2(p_{12} - p_{02})} = \frac{2\delta}{2(2-(1-f)\sqrt{2})} \approx \delta. \qquad (5)$$

5.2 Dynamic model of robot movement

To describe the dynamics of the robot's motion, we use the classical Lagrange equations of the 2nd kind:

$$\frac{d}{dt}\left(\frac{\partial T}{\partial \dot{q}_i}\right)-\left(\frac{\partial T}{\partial q_i}\right)=Q_{q_i},\ \ i=1...k, \tag{6}$$

where: k – is the number of degrees of freedom of the mechanical system; q_i – are generalized coordinates; $\dot{q}_i$ – are generalized speeds; $T(q_i, \dot{q}_i)$ is the kinetic energy of the mechanical system, which is a function of generalized coordinates and generalized velocities; Q_{qi} is the generalized force that corresponds to the gene–ralized coordinate q_i.

In this case, the system has two degrees of freedom. As generalized coordinates, we choose: the angle of rotation of the supporting leg $q_1 = \alpha(t)$; angle of rotation of the thigh of the free leg $q_2 = \gamma(t)$; the angle of rotation of the lower leg of the free leg relative to the thigh depending on the angle $\beta(t)$ of rotation of the thigh of the leg

$$\beta(t)=\gamma(t)sign(\gamma)-\alpha_o,\ \dot{\beta}(t)=\dot{\gamma}(t)sign(\gamma)=\dot{\gamma}f_1,$$

where:

$$f_1=sign(\gamma)=\begin{cases}1...\gamma>0\\0...\gamma=0\\-1...\gamma<0\end{cases}.$$

Accordingly $\dot{\alpha}$, $\dot{\gamma}$ – the generalized speeds. Angles α and γ vary within , and angle β varies within: $-\alpha_o \le \beta \le 0$.

During movement, in the presence of chambers filled with gas, the length of the supporting leg changes and its length can be calculated by the formula

$$L=\frac{L_o}{\cos\alpha} \tag{7}$$

The speed of the body of the robot is equal to the geometric sum of two speeds, namely: the speed of the upper point of the supporting leg due to its circulation around the point of contact with the surface of movement (see Figure 4, point C_1), those. $V_1 = L\dot{\alpha}=\frac{L_o}{\cos\alpha}\dot{\alpha}$, as well as the speed of the body of the robot, depends on the speed of the specified point due to a change in the length of the leg

$$V_2=\frac{dL}{dt}=\frac{L_o\sin\alpha}{\cos^2\alpha}\dot{\alpha}. \tag{8}$$

The vectors of these speeds are mutually perpen–dicular, so the speed of the robot body is found by the formula

$$V=\sqrt{V_1^2+V_2^2}=\sqrt{\left(\frac{L_o\sin\alpha}{\cos^2\alpha}\dot{\alpha}\right)^2+\left(\frac{L_o}{\cos\alpha}\dot{\alpha}\right)^2}= \\ =-\frac{L_o}{\cos^2\alpha}\dot{\alpha};\ \ (\dot{\alpha}<0). \tag{9}$$

Then the expression for the kinetic energy T_k of the robot body will have the form

$$T_k=\frac{1}{2}m_kV^2=\frac{1}{2}m_k\left(\frac{L_o}{\cos^2\alpha}\dot{\alpha}\right)^2 \tag{10}$$

where m_k is the mass of the robot body. The sum of projections of velocities V_1,V_2 equals zero: $V_1\sin\alpha - V_2\cos\alpha = 0$. Therefore, the speed of the robot body is directed only horizontally. This is an important condi–tion for the absence of vertical vibrations in the robot body. We assume that the mass of each leg m_H is uniformly distributed along the leg. The supporting leg performs a rotational movement with an angular velo–city $\dot{\alpha}$ relative to the point of contact with the moving surface, in addition, the points of the thigh and lower leg move along the leg with a speed of V_2. Then the expression for the kinetic energy of the supporting leg of the robot will be:

$$T_1=\frac{m_HL^2}{6}(\dot{\alpha})^2+\frac{1}{2}(m_c+m_g)\left(\frac{L_o\sin\alpha}{\cos^2\alpha}\dot{\alpha}\right)^2= \\ =\frac{m_H}{6}\left(\frac{L_o}{\cos\alpha}\dot{\alpha}\right)^2+\frac{1}{2}(m_c+m_g)\left(\frac{L_o\sin\alpha}{\cos^2\alpha}\dot{\alpha}\right)^2 \tag{11}$$

where m_H – is the total mass of the leg; m_c, m_g – is the masses of the thigh and lower leg, respectively.

The free leg performs a plane-parallel movement, namely: it moves forward along with the body at a speed V, the thigh turns around the point of attachment to the body at an angular speed $\dot{\gamma}$, and the lower leg, in addition, turns around relative to the thigh with an angular speed $\dot{\beta}=\dot{\gamma}sign(\gamma)=\dot{\gamma}f_1$. Then the expression for finding the kinetic energy of the free leg of the robot has the form

$$T_2=\frac{m_c}{2}\left(V^2+\frac{(L_c\dot{\gamma})^2}{3}+VL_c\dot{\gamma}\cos\gamma\right)+ \\ +\frac{m_g}{2}\left(\begin{array}{l}V^2+\frac{(L_g\dot{\gamma})^2}{3}+(L_c\dot{\gamma})^2+2VL_c\dot{\gamma}\cos\gamma+\\+L_g\dot{\gamma}f_1(V\cos(\gamma+\beta)+L_c\dot{\gamma}\cos\beta)\end{array}\right) \tag{12}$$

The total kinetic energy of the robot mechanism is $T=T_k+2T_1+2T_2$, see formulas above (10), (11), (12).

The method for obtaining differential equations of motion of a mechanical system is of a classical nature; therefore, for brevity, we note only the operations that were performed to obtain the differential equations of motion of the robot, namely: initially, the partial deri–vatives of the kinetic energy are found, which are included in equation (1). Next, the total time derivatives are calculated, and the possible increments of the movement coordinates and rotation angles of the robot's legs are specified. As a result, we obtain the formula for the generalized force:

$$Q_\gamma=2M_2i-m_cgL_c\sin\gamma-(m_H-m_c)g(2L_c\sin\gamma+ \\ +(L_H-L_c)\sin(\gamma+\beta))-2c\beta sign(\gamma) \tag{13}$$

where: M_2 – is the torque of the electric motor; g=9.81 m/s^2 – acceleration of free fall, see other designations above.

We substitute the found expressions of the derivatives mentioned above and generalized forces into equation (6), and after simplifying the intermediate expressions, we obtain a system of differential equations of robot motion (14):

$$\begin{aligned}&\ddot{\alpha}(H^2(m_k+2m_H)+2/3HL_om_H)+(H\sin\alpha)^2(m_c+m_g))+\\&+\ddot{\gamma}(HL_c\cos\gamma(m_c+2m_g)+(HL_gm_g\cos(\gamma+\beta))sign(\alpha))=\\&=\frac{\partial T}{\partial\alpha}-A+Q_\alpha;\quad \ddot{\alpha}H\cos\gamma(m_cL_c+2m_gL_g)+\\&+\ddot{\gamma}(L_s^2(2m_c/3+m_g)+L_g^2m_g\cos\beta\,\mathrm{s}ign(\alpha))=\frac{\partial T}{\partial\gamma}-B+Q_\gamma\end{aligned}\tag{14}$$

where: $H=-\dfrac{L_o}{cos^2\alpha}$; function "A" has the following form: `

$$\begin{aligned}A=&\dot{\alpha}^2(2Hh(m_k+2m_H)-2/3hL_om_H+\\&+2(H\sin\alpha)(h\sin\alpha+H\cos\alpha)(m_c+m_g))-\\&-\dot{\gamma}\dot{\alpha}h(L_c\cos\gamma(m_c+2m_g)+f_1L_gm_g\cos(\gamma+\beta))+\\&+\dot{\gamma}^2H(L_c\sin\gamma(m_c+2m_g)+f_1L_gm_g(1+f_1)\sin(\gamma+\beta));\end{aligned}$$

function "B" in equations (14) looks like this:

$$\begin{aligned}B=&-\dot{\alpha}^2h((m_c+2m_g)L_c\cos\gamma+m_gL_gf_1\cos(\gamma+\beta))+\\&+\dot{\alpha}\dot{\gamma}H((m_c+2m_g)L_c\sin\gamma+m_gL_gf_1(1+f_1)\sin(\gamma+\beta))-\\&-2\dot{\gamma}^2m_gL_cL_g\sin\beta.\end{aligned}$$

These equations make it possible to calculate the kinematic and dynamic parameters of the movement of a walking robot. Based on the solutions of differential equations (14), the numerical Runge–Kutta method in the MATLAB environment obtained graphical dependencies, which are shown below.

5.3 Robot stability conditions

To ensure the stability of a walking robot, the resultant weight forces of all parts of the robot must pass through the intersection point of the segments that connect in pairs the attachment points of two supporting legs and two free legs. If a certain horizontal force F_o acts on the body of the robot during movement, then the condition for the stability of the robot will have the form

$$Gb/2>F_oL_o\tag{15}$$

where b – is the width of the robot foot that is in contact with the moving surface. If we introduce the stability factor k, then the robot stability condition will look like

$$\frac{Gb}{2F_oL_o}\geq k\tag{16}$$

5.4 Analysis of simulation results

The construction of a dynamic model made it possible to simulate the movement of a walking robot. Below are the simulation results for the following values of the constants, namely: the mass of the upper platform m_1 = 72kg; the weight of the platform m_2=80kg; additional payload mass m_3 = 30kg; robot body mass $m_k = m_1 + m_2 + m_3$; the mass of each leg $m_H = m_1/4$; robot stability factor k=0.3; drive gear ratio i_1 = 2; knee mechanical spring stiffness C=2 Nm/rad.; robot leg length L = 0.5m; $L_o = L\cos 45^o$.

The graph in Figure 6 shows the change in the angles of rotation of the robot's leg, it's hip, and shin of the robot's leg over time, i.e., their turning speeds. As can be seen from this graph, the speed functions are non-linear throughout the entire leg movement step. This is explained by the fact that during movement, the length of the rib and lower leg is variable due to gas compression in the chambers of the piston cylinders. As a result, the function of the speed and acceleration of the whole robot is also non-linear (Figure 7).

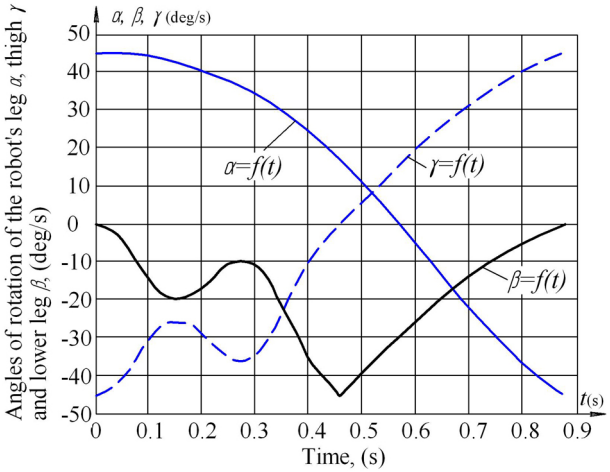

Figure 6. Change in time of the angles of rotation of the supporting leg $\alpha = f(t)$, thigh $\gamma = f(t)$, and lower leg $\beta = f(t)$

In addition, the compression of gas in the chambers of the thigh and leg under the action of the robot's weight and the expansion of gas in these chambers occur at different speeds of the pistons of these cylinders. This effect should be considered when developing a mobile robot control program.

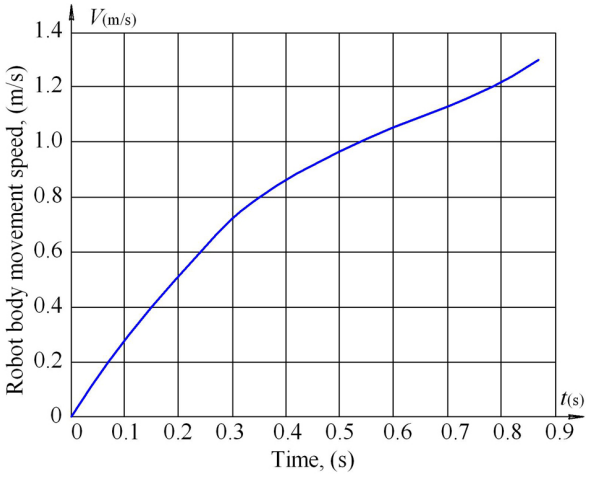

Figure 7. Graph of the change in the speed of the robot

Figure 8 shows the changes in the angular velocities of the supporting leg of the robot, i.e., when the foot is in contact with the moving surface and changing the

speed of the leg that is free from contact with the mo–ving surface. Essentially, these graphs illustrate changes in the accelerations of the drives of the supporting and free legs of the robot. Traditionally, transport mecha–nisms operate with acceleration in the range (of 1.5…2) m/s^2. For robots with wheel transmission, these values may be greater than the accelerations for walking mechanisms. Therefore, the data of the graphs in Figure 8 can be perceived as quasi-optimal. It should also be remembered that the magnitude of the accelerations of movement, combined with the mass of the moving parts, determine the inertial forces and hence the degree of stability of the robot. Therefore, when changing the direction of movement of the robot, preference should be given to lower values of the acceleration of move–ment to reduce the forces of inertia and, consequently, ensure the robot's stability.

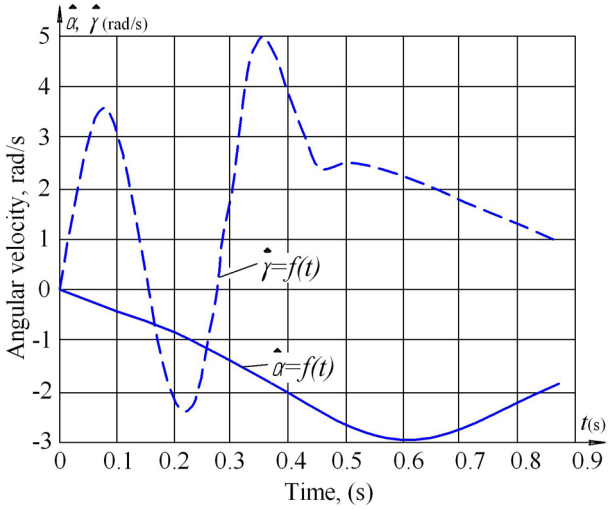

Figure 8. Changing the angular velocities of the supporting leg $\dot{\alpha}$ and thigh of the free leg $\dot{\gamma}$

5. RESULTS AND DISCUSSION

Unlike the technical solutions of walking robots discu–ssed above [2,3,6,13], which have a separate drive for each leg joint, the proposed anthropomorphic walking mechanism contains a minimum of drives for each leg. In relation to other structures considered in Section 2, the proposed walking mechanism has a significantly lower cost due to the minimization of drives and the use of sealed gas chambers for energy recovery.

Gas compression in sealed leg chambers under the action of the weight of the robot is considered an isothermal process, which corresponds to the Boyle-Mariotte law. Equations (4) and (5) make it possible to calculate the values of the initial pressure in these chambers and the lengths of the sealed chambers of the thigh and lower leg of the robot, which are necessary to perform the walking function of the robot. In addition, in order to save the resources of the robot's power sour–ces, the gas chambers, when expanding the gas and straightening the leg, perform the function of recu–perating the energy of compressed gas pressure.

As can be seen from the graph in Figure 7, the robot has sufficient movement speed for a walking mecha–nism, which, in comparison with a wheeled trans–mission, although inferior in movement speed, is supe–rior in the degree of adaptation to the moving surface. Graphs in Figure 8 show that the values of accel–erations, which determine the values of inertia forces for a certain mass of the robot, are within the accepted norms. Therefore, it is possible to guarantee the stability of the robot during movement, however, it is also nece–ssary to take into account the restrictions (15) and (16), which take into account the length of the robot's leg, the width of the foot and the weight of the robot.

6. CONCLUSION

In this article, the authors proposed a fundamentally new design of a walking mobile robot, the main dif–ference of which is the minimization of drives for each leg of the robot. This property is achieved through a combination of one electric motor, the airtight gas chambers of the thigh and lower leg of the robot, and a cable transmission from the specified motor for bending the lower leg. The gas chambers of the thigh and lower leg do not have a separate drive, and the gas in them is compressed under the action of the robot's weight. In addition, these cham–bers perform the function of recuperating the energy of the compressed gas during the extension of the legs of the robot. In addition, the presence of hydraulic dampers in the foot of the robot's foot makes it possible to compensate for and dampen shock loads when the robot walks on a surface with an arbitrary topology. Taken together, these design differences make it possible to equip each leg of the robot with only one electric motor in combination with the original kinematic scheme of the leg.

The proposed analytical and graphical dependences of the design parameters of the walking mechanism of the robot allow researchers and engineers in the field of robotics to carry out the multivariate design of such devices. The results of modeling the functioning of this robot illustrate its industrial applicability when used as a walking vehicle, and the presence of a telescopic mani–pulator on the upper platform also allows for performing technological operations, depending on the tooling of the robot's arm.

Ultimately, the proposed anthropomorphic walking robot has the ability to move on surfaces of arbitrary topology and change the trajectory of movement due to the reverse rotation of the individual platforms of its body. The main result of these studies is to reduce the cost of a walking robot by minimizing the number of en–gines and the presence of energy-recovery gas chambers.

DECLARATION OF CONFLICTING INTERESTS

The author(s) declared no potential conflicts of interest with respect to the research, authorship, and/or public–cation of this article.

REFERENCES

[1] Hafenrichte J.L., Georgeson G.E. (2019). Walking robot. Patent US 10232897. Int. Cl. B25J 15/0019. Appl. No.: 14/885360; filed: 16.10.2015; Date of Patent 19/03/2019. P. 7–9.

[2] Takahashi Hideaki, Miyazaki Susumu. Walking robot. Patent RU 2251480 Int. Cl. B25J 5/00. filed: 16.11.2001; Date of Patent 10.05.2005. Bull. No. 13.

[3] Paakkunainen Marko. Stepper device. Patent RU 2184672 Int. Cl. B62D 57/032. filed: 31.10.1996; Date of Patent 10.07.2002.

[4] Stefanov A.A., Chavdarov I.N., D.T. Nedanovski. Detailed Dynamical Model of a Simple 3D Printed Walking Robot. Seventh International Conference on New Trends in the Applications of Differential Equations in Sciences (NTADES 2020). AIP Conf. Proc. 2321, 030031-1–030031-11; https://doi.org/ 10.1063 /5.0040125.

[5] Chavdarov Ivan. 3D Printed Walking Robot Based on a Minimalist Approach. Collaborative Robots. IntechOpen. Internet resource (2021). http://dx.doi.org/10.5772/intechopen.97335

[6] T.F.C. Berninger et al. Evaluating the mechanical redesign of a biped walking Robot using experimental modal analysis. IMAC 2021 Berninger _preprint.pdf, Preprint April 2021. P. 8.

[7] Mihailo Lazarević. Optimal Control of Redundant Robots in Human-Like Fashion. FME Transactions, 2005, Vol. 33(2), pp. 53-64.

[8] Jun Huang, Duc Truong Pham, Yongjing Wang et al. A Strategy for Human-Robot Collaboration in Taking Products Apart for Remanufacture. FME Transactions, 2019, Vol. 47(4), pp. 731-738, doi: 10.5937/fmet1904731H

[9] Shevchenko A.I., Polivtsev S.O. Stepping motor of a small-sized robot. Patent UA 75991 Int. Cl. B25J 11/00. filed: 04.06.2004; Date of Patent 15.06.2006, Bull. No. 6.

[10] Mashchenko S.V., Zadnipriannyi O.M. Mobile walking robot. Patent UA 87719 Int. Cl. B25J 11/00. filed: 02.07.2007; Date of Patent 10.08.2009, Bull. No. 15.

[11] Eric R. Dunn, Robert D. Howe. Foot Placement and Velocity Control in Smooth Bipedal Walking. Submitted to the 1996, IEEE RoЬotics and Automation Conference Minneapolis, April 1996. P. 6.

[12] Tengteng Zhang and Hongwei Mo. Reinforcement learning for robot research: A comprehensive review and open issues. International Journal of Advanced Robotic Systems. May-June 2021: pp. 1–22.

[13] H. Sison, P. Ratsamee, M. Higashida et al. Generation of Inverted Locomotion Gait for Multi-Legged Robots Using a Spherical Magnet Joint and Adjustable Sleeve, 13 September 2021, PREPRINT (Version 1) available at Research Square [https:// doi.org/10.21203/rs.3.rs-892547/v1]

[14] Ilija Stevanović, Boško Rašuo. Development of a Miniature Robot Based on Experience Inspired by Nature. FME Transactions, 2017, Vol.45(1), pp. 189-197, doi:10.5937/fmet1701189S

[15] Ivan Virgala, L'ubica Miková, Tatiana Kelemenová et al. A Non-Anthropomorphic Bipedal Walking Robot with a Vertically Stabilized Base. Appl. Sci. 2022,12,4108 https://doi.org/ 10.3390/app12094108

[16] Controlled walking of planar bipedal robots. Spoelstra, M.P.A. (Author), 31 Aug. 2018, pp. 6-10

[17] Teck Chew Wee. Mechanical design and optimal control of humanoid robot (TPinokio). Journal of Engineering, 2014, Vol. 2014, Iss.

[18] Ervin Burkus, Ákos Odry, Jan Awrejcewicz et al. Mechanical Design and a Novel Structural Optimization Approach for Hexapod Walking Robots. Machines 2022, 10(6), 466; https://doi.org/ 10.3390/machines10060466

[19] Vaibhav Shrivastava, Vaibhav Diwakar, Manan Sehgal et al. Modelling and Analysis of Hexapod walking Robot. Journal of Novel Carbon Resource Sciences & Green Asia Strategy, Vol. 09, Issue 02, pp. 378-388, June 2022.

[20] Robops is equipped with a mechanical arm. Boston Dynamics. Internet resource (2022). https://naked-science.ru/community/349147

[21] Polishchuk, M., Tkach, M. Mobile robot with an anthropomorphic walking device: Design and simulation. FME Transactions, 2020, 48(1), pp. 13–20, doi: 10.5937/fmet2001013P

[22] Anthropomorphic walking device. Patent UA 125121. Int. Cl. B25J 11/00; filed: 26.12.2019; Date of Patent 12.01.2022, Bull. No. 2.

АНТРОПОМОРФНИ ХОДАЈУЋИ РОБОТ: ДИЗАЈН И СИМУЛАЦИЈА

М. Полишчук, М. Ткач, А. Стењин

Садашњу фазу развоја роботских система карак–терише употреба антропоморфних дизајна робота, чије су функције што ближе људским могућнос–тима. Овај тренд се објашњава потребом да се робо–тима дају универзалне могућности приликом изво–ђења различитих технолошких операција. У чланку се предлаже фундаментално нови дизајн ходајућег робота и описује модел његовог функционисања. Овај дизајн омогућава роботу да се креће у угаоном координатном систему, што је типично за људе. Главна мотивација за стварање оваквог робота је смањење броја погона кинематичког ланца меха–низма за ходање.

У чланку су приказани резултати математичког моделирања и препоруке за пројектовање антропо–морфних механизама за ходање. Инжењерске фор–муле и дијаграми представљени у чланку за про–рачун оптерећења силе омогућавају креирање раз–личитих модификација ходајућих робота који имају својство прилагођавања произвољној топологији површине за кретање мобилног робота. Економски ефекат се постиже смањењем броја електромотора за зглобове ногу робота и, последично, смањењем укупне цене робота који хода.